MODELING OF THE STRESS-STRAIN BEHAVIOR OF EGG SAC SILK OF THE SPIDER *ARANEUS DIADEMATUS*

Els Van Nimmen and **Kris Gellynck**:   Department of Textiles, Ghent University, Technologiepark 907, B-9052 Zwijnaarde, Belgium. E-mail: Els.VanNimmen@ UGent.be

Tom Gheysens: Department of Biology, Ghent University, K.L. Ledeganckstraat 35, B-9000 Ghent, Belgium

Lieva Van Langenhove: Department of Textiles, Ghent University, Technologiepark 907, B-9052 Zwijnaarde, Belgium

Johan Mertens: Department of Biology, Ghent University, K.L. Ledeganckstraat 35, B-9000 Ghent, Belgium

ABSTRACT.   Spider silk has attracted the attention of many scientists because of its desirable physical properties. Most of this attention has been devoted to dragline silk, a thread that has high tensile strength, high strain and ultra-low weight. To help understand structure-property relationships in spider silks, the tensile behavior of egg sac (cylindrical gland) silk of *Araneus diadematus* Clerck 1757 was compared with dragline (major ampullate gland) and silkworm silks. In addition, stress-strain curves of egg sac silk were simulated by a spring-dashpot model, specifically a Standard Linear Solid (SLS) model. The SLS model consists of a spring in series with a dashpot and in parallel with another spring, resulting in three unknown parameters. The average stress-strain curve of fibers from five different egg sacs could be accurately described by the model. Closer examination of the individual stress-strain curves revealed that in each egg sac two populations of fibers could be distinguished based on the parameters of the SLS model. The stress-strain curves of the two populations clearly differed in their behavior beyond the yield point and were probably derived from two different layers within the egg sac. This indicates that silks in the two layers of *A. diadematus* egg sacs probably have different tensile behavior.

Keywords: Spider silk, tensile behavior, cocoon, cylindrical gland, tubuliform gland, Araneidae

Spider silk has attracted considerable attention as a natural fiber in the last 10 years because spider silk, especially dragline silk, shows a unique combination of high strength, high strain and extreme fineness. The silk produced by orb-web-weaving araneid spiders provides ideal material for studying the relationships between molecular structure and mechanical properties for protein-based structural materials. Araneid spiders have seven different gland-spinneret complexes, each of which synthesizes a unique blend of structural polymers and produces a fiber with a unique set of functional properties. An overview of the different spider silks of *Araneus diadematus* Clerck 1757, their glands, their function and amino-acid composition is provided in Table 1.

Spiders produce silks that range from Lycra-like elastic fibers to Kevlar-like superfibers, but it is not known how spiders modulate the mechanical properties of silks. Table 2 gives an overview of the tensile properties of spider silks and some other biological and engineering materials.

The spider silks that have been most studied are products of the major ampullate (MA) glands. The tensile strength (or a measure of the force needed to break a material) of MA silk is clearly higher than other polymeric biomaterials such as tendon collagen and bone as can be seen in Table 2. Moreover, because of its much higher strain to break value or extensibility, its toughness (as indicated by the work to rupture value in Table 2) or the energy required to break spider silk can be ten

Table 1.—Types and functions of spider silk for *Araneus diadematus* (Andersen 1970, Kaplan 1998). Small side chains for amino acids include glycine (Gly) + alanine (Ala) + serine (Ser)−polar = aspartic acid + threonine + serine + glutamic acid + tyrosine + lysine + histidine + arginine.

Silk	Gland	Function	Amino-Acids
Dragline	Major ampullate	Orb web frame, radii, dragline	Gly (37%), Ala (18%), small side chains (62%), polar (26%)
Viscid	Flagelliform	Prey capture, sticky spiral	Gly (44%), Pro (21%), small side chains (56%), polar (17%)
Glue-like	Aggregate	Prey capture, attachment to sticky spiral	Gly (14%), Pro (11%), polar glue (49%), small side chains (27%)
Minor	Minor ampullate	Orb web frame, bridging lines	Gly (43%), Ala (37%), small side chains (85%), polar (26%)
Egg sac	Cylindrical (tubuli-form)	Reproduction	Ser (28%), Ala (24%), small side chains (61%), polar (50%)
Wrapping	Aciniform	Wrapping captured prey	Ser (15%), Gly (13%), Ala (11%), small side chains (40%), polar (47%)
Attachment	Piriform	Attachment to environ-mental substrates	Ser (15%), small side chains (32%), polar (58%)

times greater than that of other biological materials. Since initial modulus (for definition see Table 2) is a measure of stiffness, it is fair to say that spider MA silk is amongst the stiffest and strongest polymeric biomaterials known. However, the initial modulus or stiffness of MA silk is well below that of Kevlar, carbon fiber and high-tensile steel, engineering materials that are commonly employed to transmit and support tensile forces. Note also that the strength of MA silk is somewhat less than that of these engineering materials. Nevertheless, MA silk is still tougher than these engineering materials because of its large extensibility. See Table 2 for a summary of definitions concerning mechanical properties.

The viscid silk (Gosline et al. 1994) that forms the glue-covered catching spiral, is another truly remarkable spider silk material. Its initial modulus or stiffness is three orders of magnitude lower than that of MA silk and is comparable with that of a lightly cross-linked rubber. With a maximum strain of approximately 270%, viscid silk is not exceptionally stretchy compared to other rubbery materials, but its strength, at approximately 0.5 GPa, makes viscid silk roughly ten times stronger than any other natural or synthetic rubber.

Of all the silks, MA silk has been an object of desire for materials engineers because of its extreme performance properties, particularly its strength. Investigators have already been searching for more than 15 years to produce ''synthetic'' dragline silk in quantities sufficient for applications such as bullet-proof vests, parachute cords, surgical sutures and substitutes for ligaments. However, commercial production of ''synthetic'' MA silk is still not possible. We have focused on the mechanical and structural properties of spider silk of the egg sac, which to this point, is not well studied. We believe that it is precisely through correlating chemical, microstructural and consequent property differences between silks that knowledge of how the spider controls the fiber function will be acquired.

Egg sac silk is secreted by the cylindrical (= tubuliform) glands. At any point along its length, the egg sac fiber must be able to bend easily in one plane but otherwise resist bending and stretching. As reported by Barghout et al. (2001), these mechanical properties are imparted by a multiaxial anisotropic microstructure that is not observed for MA silk. Barghout et al. (1999) also observed the presence of non-periodic lattice crystals identified previously in the MA silk of *Nephila clavipes* Linnaeus 1767 (Thiel et al. 1997). Moreover, they found that these crystals in *A. diadematus* Clerck 1757 egg sac silk are twisted parallel to the chain direction in contrast to what is found for MA silk. This is suggested to be the reason for the lower stiffness that is found for *A. diadematus* egg sac silk compared to MA silk (Stauffer et al. 1994).
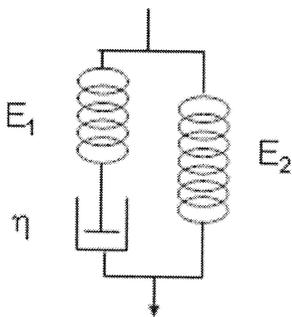
Stauffer et al. (1994) compared the physical

Figure 1.—The standard linear solid model that was used to simulate the stress-strain behavior of egg sac silk of *Araneus diadematus*.

properties of three silks (secreted by the major ampullate, minor ampullate and cylindrical glands) from *N. clavipes* and *Araneus gemmoides* Chamberlin & Ivie 1935. Comparing silks within each species, they concluded that major ampullate silk is substantially stronger than either of the other two silks. Egg sac silk is next, followed closely by minor ampullate silk. The strain of these different silks seemed comparable.

The dominant, repeated crystallizable motifs in egg sac silk of *A. diadematus* are similar to the motifs that form β-sheet crystals in MA silk spun by *N. clavipes* (Guerette et al. 1996; Thiel et al. 1997). The number of times these motifs are repeated for *Araneus* egg sac silk are however somewhat smaller than the corresponding values for *Nephila* MA silk. From the materials science viewpoint it is expected that similar primary structures at the molecular level will lead to similar ordering schemes at microstructural scales. This viewpoint is axiomatic in our use of egg sac silk to obtain further insights into the structure of MA silk. Working with *Araneus* egg sac silk offers a significant advantage relative to working with MA silk: useful amounts are produced in a convenient (compact) form.

In a previous study (Van Nimmen et al. 2003), the effects of UV-light and humidity on the stress-strain properties of egg sac silk of *A. diadematus* were demonstrated. Another study (Van Nimmen et al. 2004) considered the effect of strain-rate on the tensile properties of egg sac silk of *A. diadematus*.

The aim of the present study was to investigate how the stress-strain behavior of egg sac silk compared with the behavior of dragline silk and cocoon silk obtained from silkworms. We expected that spider egg sac and silkworm cocoon silks would have similar tensile properties because they serve similar functions (providing shelter and protection). Attention was focused on the shape of the stress-strain curves.

Mechanical properties are often characterized only by breaking force, breaking strain

Table 2.—Tensile mechanical properties of spider silks and other materials as derived from the literature (Gosline et al. 1999; Denny 1976). Initial modulus is defined as the modulus in the elastic range of the diagram in which strain changes are still reversible, it is usually calculated from the slope of the initial elastic region of the force-strain curve, also the term stiffness is used; strength (or tensile strength) is a measure for the breaking force or the force required to break the material; strain to break is the increase in length of a specimen produced by the breaking force, usually expressed as a percentage of the original length; toughness is a measure of the required energy to break a material and is calculated as the area contained by the force-strain curve up to the breaking point, often indicated as the work to rupturevalue.

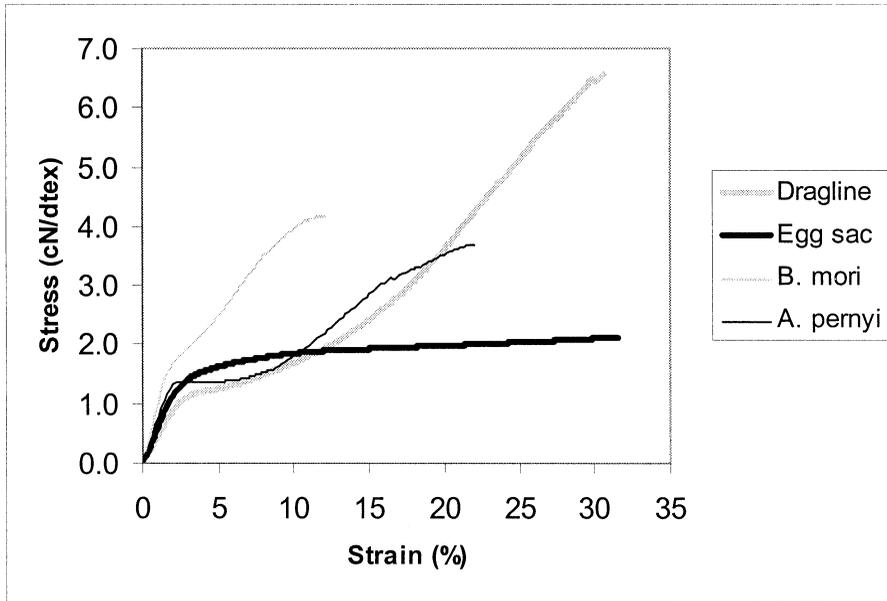| Material	Initial modulus (GPa)	Strength (GPa)	Strain to break (%)	Work to rupture (MJ m^{-3})
Araneus MA silk	10	1.1	27	160
Araneus viscid silk	0.003	0.5	270	150
Bombyx mori silk	7	0.6	18	70
Tendon collagen	1.5	0.15	12	7.5
Bone	20	0.16	3	4
Elastin	0.001	0.002	150	2
Resilin	0.002	0.003	190	4
Synthetic rubber	0.001	0.05	850	100
Kevlar 49	130	3.6	2.7	50
Carbon	300	4	1.3	25
High-tensile steel	200	1.5	0.8	6

Figure 2.—The average stress-strain curves of different silks as measured by a single-strength tester (gauge length 20 mm, testing speed 20 mm/min) based on 169 tests of *Araneus diadematus* dragline silk, 403 tests of *A. diadematus* egg sac silk, and 49 tests each of *Bombyx mori* and *Antheraea pernyi* silk.

and initial modulus. However, we are also interested in the time-dependent behavior that is also partly included in the stress-strain curves. In this study, visco-elastic models, based on spring-dashpots, are used to simulate the stress-strain behavior for spider egg sac silk. This will help to relate the mechanical and visco-elastic characteristics to the structural properties that will be investigated in further research. Finally, because of the high variability that was noted for the tensile properties within each egg sac, a cluster analysis was performed in order to find out if different fiber populations or layers could exist within an egg sac.

METHODS

General methods.—Five egg sacs of *Araneus diadematus* Clerck 1757 were collected in a bower in Belgium (Merelbeke, 51° north latitude and 3° east longitude) in autumn. One of these *A. diadematus* spiders with her egg sac is deposited as a voucher specimen in the "Zoology Museum" (UGMD 104091), Ghent University in Belgium.

Since the egg sacs were collected in their natural habitat, we expected that the measured mechanical behavior would better represent the real characteristics than if they were produced by lab-reared spiders. The egg sacs

were removed shortly after oviposition. After removing the clearly visible outer cover, one hundred fibers were gently removed at random from the inside of each egg sac, with care taken to stress the fibers as little as possible.

For the dragline samples, some *A. diadematus* were reared in the laboratory and from thirty spiders a sample of dragline thread was manually reeled off as spiders hung freely suspended in space. From every sample, ten fibers were prepared and tested.

Fibers were also tested from cocoons of the silkworms *Bombyx mori* and *Antheraea pernyi* (Tussah silk), grown at the Silk Museum of Meliskerke (The Netherlands). Since the samples we obtained were already a thorough blend of fibers of different cocoons, we decided to reduce the number of tests to 50 for both silks. All samples were kept in a conditioned laboratory of 20 °C ± 2 °C and relative humidity of 65 ± 2% for at least 24 hours before testing.

The FAVIMAT-ROBOT (Textechno) was used to analyze the tensile properties of the egg sac, cocoon and dragline fibers. It is a semi-automatic single fiber strength tester, working according to the principle of constant rate of extension (standards: DIN 51221, DIN 53816, ISO 5079). The instrument is equipped

with a balance allowing the mass to be measured at a high resolution of 0.1 mg. Moreover, this instrument includes an integrated measuring unit for linear density i.e.; mass per unit length, expressed in dtex, which equals decigrams per kilometer. This measure has the considerable advantage that the linear density, a measure for fineness, is determined simultaneously with the tensile properties. This is particularly advantageous for natural fibers. The linear density is measured according to the vibroscopic method (ASTM D 1577–BISFA 1985/1989 chapter F).

Because of the extreme fineness of dragline thread, it was unfortunately not possible to simultaneously determine the linear density of the dragline fibers. Instead, diameters of these fibers (in μm) were measured on a large number of samples with image analysis on a light microscope and the conversion was made to dtex taking into account a specific density of 1.3 g/cm^3 as reported in the literature (Vollrath & Knight 2001).

The tensile properties were tested in standardized conditions of 20 $\pm$ 2 °C and relative humidity of 65 $\pm$ 2 % with a gauge length of 20 mm, a test speed of 20 mm/min, and a pretension of 0.05 cN/dtex. For the linear density, a test speed of 5 mm/min and a pre-tension of 0.08 cN/dtex were applied.

Visco-elastic models.—*The Maxwell model:* The stress-strain curve of polymers is often mathematically described by models indicating the visco-elastic behavior of these polymers. When a material is extended by an applied force, there is, besides the elastic component, a further component whose action opposes the applied force but whose magnitude depends on the speed of extension. This second component decays relatively slowly with time. When the applied force is subsequently removed, the same component also acts to resist the internal elastic forces that bring about contraction. This time dependency of polymers is also indicated as visco-elasticity (Saville 1999). Their behavior is fitted by a visco-elastic model as the relationship between the applied stress and resultant strain contains a time-dependent element.

Most visco-elastic models consist of a combination of springs and dashpots. The spring represents the elastic solid-like behavior where Hooke's law is valid (F = Eε where F is load or force, E is elastic modulus and ε is strain), whereas the dashpot represents the time-dependent, viscous liquid-like behavior where Newton's law is valid (F = η(dε/dt) where η is the viscosity or damping constant).

In the simplest Maxwell-model (Tobolsky et al. 1951), the visco-elastic behavior of a fiber (or yarn) is described by a spring (with elastic modulus E) and a dashpot (with damping constant or viscosity η) in series. This behavior obeys the following equation (with the strain and F the force):

$$\frac{d\varepsilon}{dt} = \frac{1}{E}\frac{dF}{dt} + \frac{F}{\eta} \qquad (1)$$

This model is often used to describe stress-relaxation, a phenomenon that is observed when a polymer is extended by a given amount and then held at that extended length. If the force required to do this is monitored, it is found to rise immediately to a maximum value and then slowly decrease with time.

To use this model to describe stress-strain curves in tensile testing, we take into account a constant increase of strain with time, so that we can pose that ε = r t, with r a constant. Equation (1) then becomes:

$$r = \frac{1}{E}\frac{dF}{dt} + \frac{F}{\eta} \qquad (2)$$

with as starting condition F(0)=F$_v$, where F$_v$ is the preload, from which the following solution is obtained:

$$F(\varepsilon) = F_v + \eta r\left[1 - \exp\left(-\frac{E}{\eta r}\varepsilon\right)\right] \qquad (3)$$

Equation (3) can be written as:

$$F(\varepsilon) = F_v + A(1 - e^{-B\varepsilon}) \quad \text{with}$$

$$A = \eta r \quad \text{and} \quad B = \frac{E}{\eta r} \qquad (4)$$

This equation allows parameters A and B to be estimated by means of a non-linear regression.

The standard linear solid model: An extension of this Maxwell model is the so-called standard linear solid (SLS) model, where a linear spring in parallel is added (Fig. 1).

Taking into account this spring in equation (2) and by differentiating, equation (4) can then be written as follows:

$$F(\varepsilon) = F_v + A(1 - e^{-B\varepsilon}) + C\cdot\varepsilon \quad \text{with}$$

$$A = \eta r \quad \text{and} \quad B = \frac{E}{\eta r} \quad \text{and} \quad C = E_2 \quad (5)$$
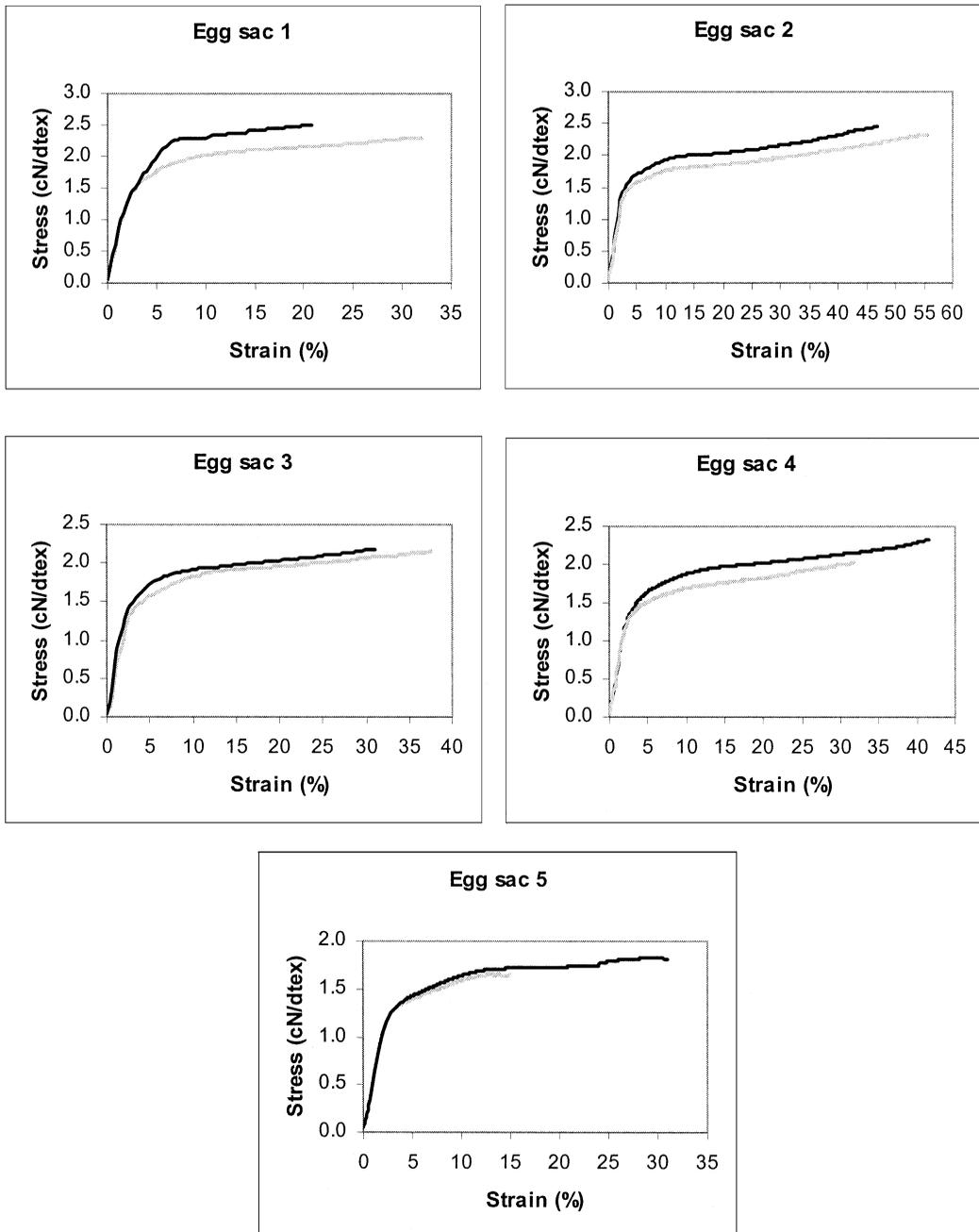
Figure 3.—Simulation by means of the standard linear solid model for two statistically different fiber populations found within an egg sac by means of a cluster analysis.

The parameters A, B and C can then be estimated by means of non-linear regression.

The Voigt model: Another time-dependent phenomenon is creep. If instead of a fixed extension, a fixed force is applied to the material, an initial extension of a magnitude is found that is expected from the force-strain curve followed by a further slow extension with time. For the description of creep or tensile testing under constant increase of load,

Table 3.—The average values (Mean) and the standard deviations (SD) of the parameters A, B and C of the SLS model for the 5 egg sacs of *Araneus diadematus* for 2 statistically different fiber populations ("1" and "2") as found by means of a cluster analysis (*n* = number of fibers within each population).

	A		B		C		
	Mean	SD	Mean	SD	Mean	SD	*n*
Egg sac 1							
1	1.84	0.14	0.46	0.05	0.015	0.010	52
2	2.39	0.20	0.36	0.06	−0.006	0.021	14
Combined	1.95	0.28	0.44	0.06	0.010	0.015	66
Egg sac 2							
1	1.75	0.05	0.50	0.05	0.013	0.003	33
2	1.58	0.04	0.51	0.07	0.012	0.001	27
Combined	1.67	0.09	0.50	0.06	0.012	0.002	60
Egg sac 3							
1	1.70	0.07	0.42	0.04	0.011	0.002	31
2	1.72	0.15	0.54	0.03	0.012	0.003	24
Combined	1.71	0.11	0.47	0.07	0.011	0.003	55
Egg sac 4							
1	1.72	0.11	0.45	0.07	0.013	0.002	43
2	1.48	0.11	0.56	0.09	0.016	0.004	29
Combined	1.62	0.16	0.50	0.10	0.014	0.004	72
Egg sac 5							
1	1.28	0.11	0.58	0.06	0.021	0.007	19
2	1.50	0.13	0.47	0.05	0.010	0.003	48
Combined	1.44	0.16	0.50	0.07	0.013	0.007	67

the simplest model used is the Voigt model. This model consists of a spring (elastic constant E) in parallel with a dashpot (with damping constant η). The visco-elastic behavior is then described by the following differential equation (with ε the strain and F the force):

$$F = E\varepsilon + \eta\frac{d\varepsilon}{dt} \qquad (6)$$

Using the correct starting conditions for creep or tensile testing under constant increase of load, solutions for this equation can be found. Since these are not valuable for this study, the reader is referred to the literature (Saville 1999).

Other visco-elastic models: The models described above can be extended to more elements, such as the "four-elements model" consisting of a Maxwell-element in series with a Voigt element or more generalized Maxwell and Voigt models considering a finite or infinite number of Maxwell or Voigt elements connected in parallel or in series. Since it is beyond the scope of this study, the reader is again referred to the literature for further description (Saville 1999).

RESULTS

The tensile behavior of silks.—First, it should be remarked that although 500 egg sac fibers and 300 dragline fibers were tested, not all were successful mostly due to the fineness of the fiber. For the calculation of the average stress-strain curves, for which the shape is the most important, only curves with strain to break values higher than 10% were considered. The curves were stopped at the average strain to break values of all available tests. It can be expected that the measurements show a small error since probably the weakest fibers could not be tested. However, from the histogram of the strength values, the contribution of stronger fibers is not higher than that of the weaker fibers In addition, the high variability in the stress-strain curves among the different egg sacs should be noted, which can also be found in the literature on dragline silks (Madsen et al. 1999; Garrido et al. 2002).

Fig. 2 shows the average stress-strain curves of the different silks of *A. diadematus* (dragline, egg sac), *B. mori* and *A. pernyi*. It is clear that egg sac silk shows a completely different stress-strain behavior from dragline silk and even the functionally comparable silkworm cocoon silks. All stress-strain curves start with a small elastic region. For the dragline, *B. mori* and *A. pernyi* fibers, this region is followed by a plastic region and finally by strain hardening where the stress again linearly increases with strain. However spider egg sac silk shows a plastic-hardening region that is extremely flat. Since in this region the stress increases again linearly with strain, we will simply use the term "hardening region" to indicate this region.

Although egg sac silk shows about the same strain to break as dragline silk, the tensile strength of dragline silk is three to four times higher. The initial modulus (calculated from the slope of the initial straight line portion), which is a measure of stiffness of the fiber, is significantly higher for egg sac silk than for dragline thread (67 cN/dtex versus ±47 cN/dtex) ($P < 0.001$).

Simulation of tensile behavior of egg sac silk.—For this research, the stress-strain data of the five egg sacs were used, from which the average stress-strain curve shown in Fig. 2 was produced. Since we were working with tensile testing with constant increase of extension, the Maxwell-model as described earlier was used to describe the stress-strain behavior. Starting from equation (4), the parameters A and B were estimated by means of a non-linear regression. We concluded that the Maxwell-model does not completely satisfy the simulation of the stress-strain curve for the egg sac silk fibers.

We then applied the SLS model, in which the 3 parameters A, B and C of equation (5) were estimated by means of a non-linear regression. With the average data of the stress-strain curves, for each egg sac a correlation of higher than 99% with a relative error (defined as ($F_{experimental} - F_{predicted}$)/$F_{experimental}$) smaller than 0.1% was observed, except in the initial elastic region where the maximum relative error at about 0.4–0.5% strain exceeds 0.4% to 1%.

To get an indication of the variability within the egg sac, the non-linear regression was repeated for each of the individual stress-strain curves of the 100 fibers that were tested for each of the five egg sacs. Because of the observed high variability, we performed a cluster analysis (with the statistical software SPSS) on the estimated parameters A, B and C in order to identify statistically different clusters or fiber populations.

The result of this cluster analysis is given in Table 3. Within the different egg sacs, two clusters (indicated as "1" and "2") of statistically different fiber populations could be detected. In this analysis, clusters of less than 10 fiber data were removed. The clusters or fiber populations for egg sac 1, egg sac 4 and egg sac 5 show completely different A, B and C values. In other words, the level of the more horizontal hardening region (indicated by A), the shape of the yield (or transition) region (indicated by B) and the slope of the hardening region (indicated by C) of their stress-strain curves are significantly different. For egg sac 2, only the A-values of the clusters are significantly different, while the confidence regions of the parameters B and C are overlapping. With respect to egg sac 3, the B-values of the clusters are significantly different, while the confidence regions of the parameters A and C are overlapping.

Based on the cluster analysis, the stress-strain curves of the individual fibers from each egg sac were split into 2 groups and the average curve of each group was calculated. These average stress-strain curves based on the two different fiber populations for each egg sac are shown in Fig. 3. It can be concluded that the fiber populations seem to differ mostly in the level of the relatively flat so-called hardening region and thus the breaking stress value. The initial modulus and the modulus of the hardening region, i.e. the tangent modulus at the yield point, seem to be quite equal for both fiber populations.

DISCUSSION

The tensile behavior of silks.—The shapes of the stress-strain curves that we found and that were also seen by Van Nimmen et al. (2004) are similar to those that were found by Stauffer et al. (1994). However, Stauffer et al. 1994 determined different absolute values for strength and strain. As their testing procedures were different from our, it is difficult to evaluate the discrepancies. They found for *Araneus gemmoides* MA silk final breaking points

at extensions of about $15 \pm 2\%$ ($n = 10$) with a final stress of 4.7 ± 0.5 GPa and for egg sac silk breaking strains at $19 \pm 2\%$ ($n = 10$) with tensile strengths of 2.3 ± 0.2 GPa. They obtained much higher stress values than found elsewhere for MA silk (see Table 2) because, for diameter measurements, they took into account the ten smallest diameter points in several sections of the silks. With respect to strain, we found much higher values ($30 \pm 9\%$, $n = 183$) for MA silk and $32\% \pm 16\%$, $n = 398$ for egg sac silk), with a much higher variability, probably due to the greater number of tests performed. It is not clear if this difference is due to the difference in testing procedure or to the spider species. However, other published data of MA *Araneus* silk mention a strain to break value of 27% (Denny 1976) which agrees better with our strain data. In order to make further comparisons possible with the tensile properties presented in Table 2, our breaking stress and stiffness values were converted to the GPa unit, taking into account a specific density of 1.3 g/cm^3 (Vollrath & Knight 2001). The breaking stress values thus obtained were 0.94 ± 0.36 GPa ($n = 183$) for MA silk and 0.27 ± 0.05 GPa ($n = 398$) for egg sac silk.

The stiffness values, calculated from the slope of the initial elastic region, resulted in values for MA silk of 6.1 ± 2.4 GPa ($n = 167$) and for egg sac silk of 8.7 ± 0.9 GPa ($n = 434$). The stiffness value for MA silk seems low compared to the value of 10 GPa that is given in Table 2. Probably the testing conditions play a role in this difference (forced or unforced silking, single or multifilament, climate, strain rate, gauge length, etc). Denny's (1976) analysis of the strain-rate dependence of MA silk demonstrated that the initial stiffness increases from 9.8–20.5 GPa when the strain rate is increased from 0.0005 s^{-1} to 0.024 s^{-1}. Also the spinning conditions (e.g. drawing speed, body temperature) have been reported to affect the tensile properties (Vollrath et al. 2001).

We believe the different stress-strain behavior of dragline and egg sac silk is partly due to different amino acid compositions. Glycine (Gly) and alanine (Ala) are most abundant in draglines, while serine (Ser) and Ala are most abundant in egg sac silk (Table 1). Moreover, the proline rich motif Gly-Pro-Gly-X-X occurs in dragline silk but not in egg sac silk

(Guerette et al. 1996; Gosline et al. 1999). Thiel et al. (1997) believe that the structure of the proline residue forces a severe kink in an extended backbone chain. On the other hand, the total content of the small amino acids Gly, Ala and Ser, which is usually taken as an indication of crystal forming potential (Gosline et al. 1986), is almost the same for dragline and egg sac silk (Table 1). Thus, we would expect the crystallinity of both fibers to be similar. However, in tensile testing, the weakest regions, i.e. the more amorphous regions, most affect the stress-strain behavior. Consequently, two silks with similar crystallinity may exhibit dissimilar tensile properties. Thus, the different stress-strain curves of MA and egg sac silk are probably more a reflection of differences in the arrangement (chain lengths, number of coils, etc.) of the structural elements of the amorphous regions than of the crystalline domains.

Since glycine is the simplest amino-acid (side group H), while serine is an amino-acid with a much more voluminous side group (CH_2OH), the difference in strength between dragline and egg sac silks may be mainly attributed to the more compact structure which can be built with glycine, resulting in a structure that is more resistant to stress. Although the structure of the glycine-rich regions of MA silk is imperfectly understood, there is consensus that these regions are part of a more oriented amorphous phase (Jelinski et al. 1999; van Beek et al. 2002). Moreover, the proline-rich regions in MA silk are expected to include more turns, resulting in a higher number of hydrogen bonds and thus in a more stress resistant structure. A more intensive study of the spinning process, structure and morphology of spider silk, especially egg sac silk, is required to further explain the difference in tensile behavior.

We also note that the shapes of the stress-strain curves obtained for the silkworm silks are more similar to dragline silk than to egg sac silk, even though the silkworm and spider use the former two silks for completely different functions. Since the main constituents of *B. mori* and *A. pernyi* silks are also glycine and alanine (44% Gly, 29% Ala, 12% Ser in *B. mori* and 27% Gly, 43% Ala, 11% Ser in *A. pernyi* (Kishore et al. 2002)), the higher similarity in behavior to dragline silk could be expected.

Simulation of tensile behavior of egg sac silk.—The different fiber populations vary mostly in the hardening region, that is, the region beyond the yield point. The initial elastic region, and the modulus of this region, that is usually used to define the stiffness, appears not to differ for the two fiber populations. As mentioned before, the spring in the SLS model represents the solid character whereas the dashpot indicates the liquid character. By adding a (elastic) spring to the Maxwell model, an element is added that results in a linear relation between stress and strain beyond the yield point. The significance of the coefficient C indicates that there is indeed a significant, although small, increase in stress as a function of strain beyond the yield point. During post-yield extension, the long molecules tend to become oriented along the stress axis and, as a result, a structure may be obtained which approaches that of a crystalline material. This is, in fact called ''strain-induced crystallization'' (Wainwright et al. 1976) and leads to a notable increase in the value of the instantaneous elastic modulus. A link with the twisted non-periodic lattice (NPL) crystals demonstrated by Barghout et al. (1999) can be made. The twist of these regions may result in the flattened behavior beyond the yield point, i.e. the lower tangent modulus at the yield point, for egg sac silk compared to dragline silk (in which the twist of the NPL crystals is not observed).

Since the fibers were randomly selected from each egg sac, the two fiber populations can probably be attributed to different layers that constitute the egg sac. Our own preliminary structural research of the egg sac of *Araneus diadematus* indeed confirms the existence of different layers, especially observed as a slight difference in color and in the stacking of the fibres above and below the eggs. Different layers in the egg sac structure are also found for the spider *Zygiella x-notata* (Gheysens et al. in press). A more detailed study in which an attempt is made to divide the different layers will be required to confirm this.

This study has shown that egg sac silk of *Araneus diadematus* has a completely different tensile behavior from dragline of the same spider. In contrast to what was expected given the functions of the different silks, more similarities were found between spider dragline silk and cocoon silks of *Bombyx mori* and *Antheraea pernyi* than between the latter and the spider egg sac silk. We suggest that the difference in stress-strain behavior is partly due to the different amino acid composition, and especially the structure of the amorphous domains. A further structural and morphological study of egg sac silk is required to further explain its special stress-strain behavior.

The stress-strain curve of spider egg sac silk can be accurately simulated by the standard linear solid model with 3 parameters to be estimated. A more detailed analysis of the estimated parameters A, B and C revealed that for each egg sac two clusters or populations of fibers could be found, mostly differing in the stress level of the region beyond the yield point. Since the fibers were taken randomly from each egg sac, it is suggested that the different behavior of the two fiber populations is due to the different tensile behavior of two layers constituting an egg sac. A further study will be required to relate the mechanical properties to the functions of these different layers.

LITERATURE CITED

Andersen, S.O. 1970. Amino Acid Composition of Spider Silks. Comparative Biochemistry and Physiology 35:705–711

Barghout, J.Y.J., B.L. Thiel, C. Viney. 1999. Spider (*Araneus diadematus*) cocoon silk: a case of non-periodic lattice crystals with a twist? International Journal of Biological Macromolecules 24: 211–217.

Barghout, J.Y.J., J.T. Czernuszka, C. Viney. 2001. Multiaxial anisotropy of spider (Araneus diadematus) cocoon silk fibres, Polymer 42:5797–5800.

Denny, M. 1976. The physical properties of spider's silk and their role in the design of orb-webs. Journal of Experimental Biology 65:483–506.

Garrido, M.A., M. Elices, C. Viney, J. Pérez-Rigueiro. 2002. The variability and interdependence of spider drag line tensile properties. Polymer 43:4495–4502.

Gheysens T., L. Beladjal, K. Gellynck, E. Van Nimmen, L. Van Langenhove, J. Mertens. In press. Cocoon construction of the *Zygiella x-notata* (Arachnida, Araneidae). Journal of Arachnology.

Gosline, J.M., M.E. DeMont, M.W. Denny. 1986. The structure and properties of spider silk. Endeavour, New Series 10:37–43.

Gosline, J.M., C.C. Pollak, P.A. Guerette, A. Cheng, M.E. Demont, M.W. Denny. 1994. Elastomeric Network Models for the Frame and Viscid Silks from the Orb Web of the Spider Araneus diadematus. Pp. 328–341. *In* Silk Polymers: Material

Science and Biotechnology. (D. Kaplan, W.W. Wade, B. Farmer. & C. Viney, eds) ACS Symposium Series 544, Washington DC.

Gosline, J.M., P.A. Guerette, C.S. Ortlepp, K.N. Savage. 1999. The mechanical design of spider silks: From fibroin sequence to mechanical function. Journal of Experimental Biology 22:3295–3303.

Guerette, P.A., D.G. Ginzinger, B.H.F. Weber, J.M. Gosline. 1996. Silk properties determined by gland specific expression of spider fibroin gene family. Science 272:112–114.

Jelinski, L.W., A. Blye, O. Liivak, C. Michal, G. LaVerde, A. Seidel, N. Shah, Z. Yang. 1999. Orientation, structure, wet-spinning, and molecular basis for supercontraction of spider dragline silk. International Journal of Biological Macromolecules 24:197–201.

Kaplan, D.L. 1998. Fibrous proteins—silk as a model system. Polymer Degradation and Stability 59:25–32.

Kishore, A.I., M.E. Herberstein, C.L. Craig, F. Separovic. 2002. Solid-state NMR Relaxation Studies of Australian spider silks. Biopolymers 61: 287–297.

Madsen, B., Z.Z. Shao, F. Vollrath. 1999. Variability in the mechanical properties of spider silks on three levels: interspecific, intraspecific and intraindividual. International Journal of Biological Macromolecules 24:301–306.

Saville, B.P. 1999. Physical testing of textiles; Woodhead Publishing Ltd., ISBN 1 85573 367 6.

Stauffer, S.L., S.L. Coguill, R.V. Lewis. 1994. Comparison of physical properties of three silks from Nephila Clavipes and Araneus Gemmoides. Journal of Arachnology 22:5–11.

Thiel, B.L., K.B. Guess, C. Viney. 1997. Non-periodic lattice crystals in the hierarchical microstructure of spider (major ampullate) silk. Biopolymers 41:703–719.

Tobolsky, A.V., B.A. Dunell, R.D. Andrews. 1951. Stress relaxation and Dynamic properties of polymers. Textile Research Journal 21:404–411.

van Beek, J.D., S. Hess, F. Vollrath, B.H. Meier. 2002. The molecular structure of spider dragline silk: Folding and orientation of the protein backbone. Proceedings of the National Academy of Sciences 99(16):10266–10271.

Van Nimmen, E., P. Kiekens, J. Mertens. 2003. Some material characteristics of spider silk; International Journal of Materials & Product Technology 18:344–355.

Van Nimmen, E., K. Gellynck, L. Van Langenhove, J. Mertens. 2004. The difference in tensile behavior of different silks of the spider *A. diadematus*. Pp. 503–512. *In* Design and Nature II: Comparing design in nature with science and engineering. (M.W. Collins & C.A. Brebbia, eds.). WIT Press, United Kingdom (ISBN 1-85312-721-3).

Vollrath, F. and D. Knight. 2001. Liquid crystalline spinning of spider silk. Nature 410:541–48.

Vollrath F., B. Madsen, Z. Shao. 2001. The effect of spinning conditions on the mechanics of a spider's dragline silk. Proceedings of the Royal Society of London Series B Biological Sciences 268:2339–2346.

Wainwright S.A., W.D. Biggs, J.D. Currey, J.M. Gosline. 1976. Pp. 33–41. *In* Mechanical Design in Organisms. Edward Arnold (Publishers) Limited. London. ISBN 07131 2502 0.